Chemical Alterations Induced by Rock–Fluid Interactions When Injecting Brines in High Porosity Chalks

Transport in Porous Media

ISSN 0169-3913
Volume 87
Number 3

Transp Porous Med (2011)
87:679-702
DOI 10.1007/
s11242-010-9708-3

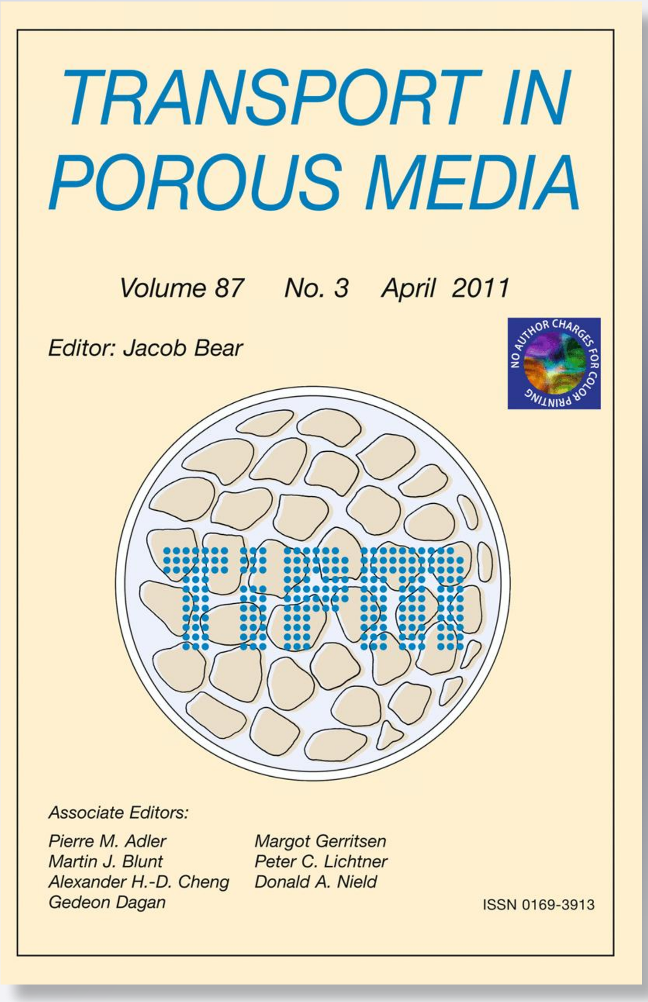

Transp Porous Med (2011) 87:679–702
DOI 10.1007/s11242-010-9708-3

Chemical Alterations Induced by Rock–Fluid Interactions When Injecting Brines in High Porosity Chalks

M. V. Madland · A. Hiorth · E. Omdal · M. Megawati · T. Hildebrand-Habel · R. I. Korsnes · S. Evje · L. M. Cathles

Received: 15 December 2009 / Accepted: 23 December 2010 / Published online: 8 January 2011

Abstract Effect of the aqueous chemistry on the mechanical strength of chalk has extensively been studied during the last decade. At high temperatures (~130°C), chalk exposed to seawater is significantly weaker compared to chalk exposed to distilled water when considering the hydrostatic yield strength and the following creep phase. The explanation of these experimental results must be of a chemical nature, as the density and viscosity of the aqueous phase vary little among these different brines. We present the results from simplified aqueous chemistry using $MgCl_2$ brines, and compare these results with seawater. Previous studies show that different ions, e.g. Ca^{2+}, Mg^{2+}, ${SO_4}^{2-}$ in the injected brine, as well as the chalk mineralogy have an impact on the stability of the rock. We performed mechanical tests on chalk cores from Liège and Stevns Klint; it was found that these two outcrop chalks exhibit an unexpected difference in their mechanical responses when comparing cores flooded with NaCl and $MgCl_2$ at 130°C. The results of this study show that the effects of magnesium seem to be governed not only by the differences in mineralogy, but also a time dependency on chalk deformation is additionally observed. Independent of the chalk type tested, the chemical analyses performed show that when $MgCl_2$ is flooded through the core, a significant loss of magnesium and a considerable additional amount of calcium are detected in the effluent. The experimental observations fit very well with the time-dependent chemical changes gained from the mathematical model of this study that accounts for transport effects (convection and molecular diffusion) as well as chemical processes such as precipitation/dissolution. Based on the calculations and chemical analyses, we argue that the loss of magnesium and the production of calcium cannot solely be a consequence of a substitution process. The calculations rather indicate that magnesium is precipitated forming new mineral

---

M. V. Madland (✉) · A. Hiorth · E. Omdal · M. Megawati · R. I. Korsnes
Department of Petroleum Engineering, University of Stavanger, 4036 Stavanger, Norway
e-mail: merete.v.madland@uis.no

A. Hiorth · T. Hildebrand-Habel · S. Evje
International Research Institute of Stavanger, IRIS, P.O. Box 8046, 4068 Stavanger, Norway

L. M. Cathles
Department of Earth and Atmospheric Sciences, Cornell University, Ithaca, NY, USA

phases and in this process not only calcite, but also silicates are dissolved. The amount of dissolved calcium and silicon from the rock matrix is significant and could thus cause an additional deformation to take place. Both the retention of magnesium in the chalk core and the formation of newly precipitated magnesium-bearing carbonates and/or magnesium-bearing clay-like minerals after flooding with $MgCl_2$ brine were demonstrated using scanning electron microscopic methods. In addition, precipitation of anhydrite as a result of flooding with seawater-like brine was proven. The water-induced strain not only depends on the ion composition of the injected brine; moreover, the presence of non-carbonate minerals will most likely also have a significant influence on the mechanical behaviour of chalk.

Keywords Chalk · Water weakening · Mechanical tests · Chemical analyses · Modelling · Mineral dissolution/precipitation

1 Introduction

The compaction of chalk reservoirs is experienced at the Ekofisk field, and is not only a result of an increase in effective stresses linked to pore pressure depletion during oil recovery. There is, however, an additional impact of the seawater injection when water replaces oil in chalks: it causes enhanced compaction of the rock, which was further shown to induce additional seabed subsidence. The phenomenon is referred to as the water-weakening effect on chalks.

The chalk–fluid interactions were shown to be strongly influenced by variations in testing temperature. The chemical effects of seawater-like brines, Ekofisk formation water and distilled water on the mechanical properties of high porosity outcrop chalks have been extensively studied (e.g. Korsnes 2007; Korsnes et al. 2006a, b, 2008; Madland 2005; Madland et al. 2008; Zangiabadi et al. 2009). These rock mechanical and pure core flooding studies at elevated temperatures both on high and lower porosity chalks from quarries of either Stevns Klint, Rørdal, Lixhe or Kansas have in general shown that the chemical composition of the saturating and flooding fluid has crucial influence on the mechanical strength of the chalk. Apparently, the presence of sulphate ions in the seawater-like brines caused a significant weakening of the chalk framework, especially as the testing temperature was increased. The chemical weakening of chalk by seawater-like brines appeared to take place when Mg^{2+} ions in solution substituted Ca^{2+} ions at the intergranular contacts in the presence of ${SO_4}^{2-}$ ions (see Korsnes et al. 2006a, b, 2008). It was also proposed that this weakening process increased with increasing temperature. The suggested mechanism does not, however, explain some of the recently reported results on Kansas chalk (Madland et al. 2008; Zangiabadi et al. 2009), which showed an enhanced weakening as cores were exposed to seawater without magnesium at 90°C. Apparently, in this case no substitution of Ca^{2+} by Mg^{2+} could take place as magnesium was not present in the brine. In light of these new results, other possible mechanisms, such as surface charge and dissolution of the core material, should be considered.

The aim of this study is thus to investigate the effect of individual ions by simplifying the aqueous chemistry. In particular, we repeat some of the rock mechanical tests performed, and additionally reduce the complexity of the aqueous brine by using distilled water and solutions containing solely NaCl or $MgCl_2$. The impact of non-carbonate minerals originally present in the chalk is also addressed, highlighting the importance of selecting an adequate representative onshore rock substitute when studying the mechanisms behind the water-weakening phenomenon observed in reservoir chalks.

From the previous experimental and modelling studies dealing with water-induced compaction and wettability alteration in chalks (Heggheim et al. 2005; Hiorth et al. 2008a, b; Korsnes et al. 2006a, b, 2008; Madland 2005; Madland et al. 2008; Zangiabadi et al. 2009), it is obvious that three ions are of particular importance when chalk cores are exposed to seawater-like brines at increased temperatures: Mg^{2+}, Ca^{2+}, and $SO_4{}^{2-}$. The published research so far, however, emphasizes the complexity of the systems tested. Therefore, a need to simplify the system has been identified and each ion of importance will thus be studied individually. Within this study, the role of Mg^{2+} is specifically studied and discussed in detail from both an experimental as well as a modelling points of view. The interaction of Mg^{2+} with the chalk framework also seems to be strongly influenced by the presence of other minerals such as silicates and is therefore further studied by comparing test results obtained from two different outcrop chalks.

2 Chemical Aspects and Theories

One of the suggested theories regarding water weakening of chalk is the so-called substitution process taking place inside the chalk when seawater-like brines are injected at high temperatures (Korsnes et al. 2006a, b, 2008). This proposed mechanism was explained in terms of Mg^{2+} in the aqueous phase substituting Ca^{2+} at intergranular contacts, provided that $SO_4{}^{2-}$ is present. To evaluate this hypothesis, it is of importance to quantify the ions. We are therefore in particularly interested in the following:

- By analysing the effluent composition, the amount of magnesium lost inside the core can be calculated. Is this number larger than the number of calcium sites available at the grain surfaces?
- Since magnesium ions are smaller than calcium ions, an increase in the compaction rate should be observed upon substitution. When all calcium available at the grain surfaces is substituted by magnesium, the substitution process should stop and no additional compaction should then be observed.

The amount of calcium available for substitution can be calculated by assuming that the values in Table 1 are valid for the cores used in the experiments.

From the data presented in Table 1, the number of adsorption sites can be calculated from

$$N_\sigma = \frac{1}{4} s\rho(1-\phi)\frac{\pi D^2 L}{N_\mathrm{A}} = 1.9 \times 10^{-3}\,\mathrm{mol}. \tag{1}$$

The maximum number of adsorption sites in this core is thus 0.0019 mol. When these sites are exchanged, the substitution process should stop or at least be significantly slowed down.

Table 1 Values used for estimating the number of available adsorption sites in the chalk cores

Length of core (L)	7 cm
Diameter of core (D)	3.7 cm
Specific surface area (s)	2000 m^2/kg
Porosity (ϕ)	0.42
Density of rock (ρ)	2600 kg/m^3
Adsorption sites (σ)	5 sites/$(nm)^2$ (Davis and Kent 1990)
Avogadro's number (N_A)	6.022×10^{23} mol^{-1}

The values listed are typical values for the cores used in this study

This is because a deeper substitution process inside the grains requires that the substituted layer at the surface needs to diffuse deeper into the grain; solid-state diffusion is regarded as a very slow process.

3 Experimental Procedures

3.1 Core Material, and Saturating and Flooding Fluids

Outcrop chalk from the quarries of Lixhe near Liège in Belgium and Stevns Klint near Copenhagen in Denmark was used in the experimental work. The main characteristics of these outcrop chalks are Liège chalk: late Campanian age, porosity from 40 to 43%, permeability 1–2 mD; Stevns Klint chalk: Maastrichtian age, porosity from 42 to 50%, permeability 1–2 mD. The Liège chalk is composed of >98 wt% $CaCO_3$ and <2 wt% other non-carbonate minerals, whereas for Stevns Klint the non-carbonate content is typically 0.2 wt% (Hjuler and Fabricius 2009). The chalks were cored and the cylindrical samples machined to the desired diameter of 37 mm and subsequently cut into a length of about 70–80 mm. After shaping, the cores were dried for 24 h at 130°C in a drying furnace, and weighed before they were saturated with distilled water in a vacuum vessel. The cores' porosities were determined by comparing the cores' dry and saturated weights.

Six different fluids were used during the experimental work: distilled water (DW), 0.657 M NaCl, 0.1095 M $MgCl_2$, 0.219 M $MgCl_2$, synthetic seawater (SSW), and SSW with lower NaCl content. The brines used, except for the one with 0.1095 M $MgCl_2$ and SSW with lower NaCl content, have an ionic strength similar to that of seawater. The ion composition of each of the brines is summarized in Table 2.

3.2 Equipment and Mechanical Test Procedure

The purpose of this study is not to simulate any water injection into North Sea chalk reservoirs at real in situ stress conditions, but rather to select a repeatable type of test to further study and thus improve the approach towards a more in-depth understanding behind the mechanisms

Table 2 Composition of brines injected during mechanical tests

Ions	0.657 M NaCl (mol/l)	0.1095 M $MgCl_2$ (mol/l)	0.219 M $MgCl_2$ (mol/l)	SSW (mol/l)	SSW low NaCl conc. (mol/l)
$HCO_3{}^{-a}$	0.000	0.000	0.000	0.002	0.002
Cl^-	0.657	0.219	0.438	0.525	0.125
$SO_4{}^{2-}$	0.000	0.000	0.000	0.024	0.024
Mg^{2+}	0.000	0.109	0.219	0.045	0.045
Ca^{2+}	0.000	0.000	0.000	0.013	0.013
Na^+	0.657	0.000	0.000	0.450	0.050
K^+	0.000	0.000	0.000	0.010	0.010
Ion strength	0.657	0.329	0.657	0.657	0.257
TDS (g/l)	38.40	10.42	20.84	33.39	10.01

[a] From the pH measurements of the distilled water (5.9), we have estimated the total carbonate content to be of the order 10^{-5} mol/l

causing the water weakening of chalks. Hydrostatic tests followed by creep with continuous flooding of various fluids, at an injection rate equal to either 1 or 2 pore volume per day (PV/day), were performed at low (0.7 MPa) and high (40 MPa) pore pressure in a standard hydraulically operated triaxial cell. The cell was equipped with a heat regulating system, keeping the temperature constantly at 130 ± 0.2°C during the experiments. To avoid boiling at temperatures above 100°C, a pore pressure of 0.7 MPa was applied prior to the heating of the system. The axial displacement was measured by an outside linear voltage displacement transducer (±0.05 mm) that follows the movement of the piston.

Prior to the mechanical testing, each chalk core was saturated with DW and thereafter mounted in the triaxial cell. While cleaning the cores by flooding a minimum number of 2 PVs of DW, the confining (isotropic) pressure, σ_{iso}, and pore pressure, P_{P}, were simultaneously increased to a differential stress equal to 0.5 MPa ($\sigma_{\text{iso}} = 1.2$ MPa and $P_{\text{P}} = 0.7$ MPa) and 0.7 MPa ($\sigma_{\text{iso}} = 1.4$ MPa and $P_{\text{P}} = 0.7$ MPa) for the Liège and Stevns Klint cores, respectively. Cleaning by flooding with DW was done to ensure a clean pore system, as different ions may be present due to natural pollutions originating from the location of the outcrop (Puntervold et al. 2007). In general, the cores from the two outcrops have followed a similar test procedure; however, some differences exist and will thus further be described. It should, however, be mentioned that these differences are not believed to have any significant influence on the final results obtained from the experiments carried out.

Cleaning of the Stevns Klint cores, which were prepared for both low and high pore pressure testings, took place from the very beginning, i.e. while increasing the temperature. When the testing temperature of 130°C was reached, flooding of the actual brine started. For the Liège cores, on the other hand, the cleaning with DW was fulfilled prior to any heating of the cell. After cleaning, flooding of the respective fluid was started and the triaxial cell was heated to the chosen test temperature of 130°C. Both the Liège and Stevns Klint cores were then left over night to equilibrate at a constant flooding rate of either 1 or 2 PV/day. The following day, the samples tested at low pore pressure (0.7 MPa) were isotropically loaded beyond yield, which is the point of initiation of pore collapse or where the observed stress–strain curve departs from the linear trend. Thereafter, the cores were left to creep at an effective stress level of 10.5 MPa for the Liège and 11.3–12.0 MPa for Stevns Klint cores.

Concerning the Stevns Klint cores prepared for high pore pressure testing, the building of in situ confining or total isotropic pressure and pore pressure started after the testing temperature of 130°C was reached and with continuous flooding of DW. The total isotropic stress was increased to 41 MPa meanwhile the pore pressure reached a value of 40 MPa, i.e. increasing the window from 0.7 to 1 MPa in order to minimize the risk for any leakages at these high pressure values. DW was still used as pore fluid within this pressure build-up phase. After the initial state of $\sigma_{\text{iso}} = 41$ and $P_{\text{P}} = 40$ MPa was established, the cores were all flooded with their respective testing brine, and thereafter left overnight to equilibrate at a constant flooding rate of 2 PV/day. From all the tested cores, the flooding effluent was continuously fractioned during the entire test period and analysed using an ion chromatograph (IC). Additional effluent samples from tests using both types of outcrop chalk were submitted to a commercial laboratory for analysis.

4 Results

In total 14 chalk cores were mechanically tested either at low pore pressure (7 Liège and 4 Stevns Klint cores) or high pore pressure (3 Stevns Klint cores) with continuous flooding of either DW, NaCl, SSW, SSW with low NaCl concentration or $MgCl_2$ with two different molar concentrations. All cores were hydrostatically or isotropically loaded beyond yield and thereafter left to creep at a constant stress level of 10.5 and 11.3–12.0 MPa for the Liège and Stevns Klint cores, respectively. Sampling of the effluent was continuously conducted during the hydrostatic phase as well as during the following creep phase. The fractioned effluent was chemically analysed to quantify any chemical changes of the core material.

4.1 Mechanical Tests

4.1.1 Liège Cores

The Liège cores are all labelled using RL followed by a number, e.g. RL8, RL2, etc. Table 3 lists the cores that had been tested, together with porosity, aqueous chemistry of the testing brine as well as the hydrostatic yield point. The porosity values of all samples lie in the range of 41.1–41.4 %. One core (RL2) was flooded with a 0.219 M $MgCl_2$ brine that had an ionic strength similar to that of seawater. In addition, two other cores, RL5 and RL16, were flooded with a 0.1095 M $MgCl_2$ solution, which corresponds to half the ionic strength of seawater. As seen from Table 3, the values of hydrostatic yield strength, σ_h, are ranging from 6.6 to 8.1 MPa. The core flooded with SSW (RL8) had the lowest yield point, $\sigma_h = 6.6$ MPa, followed by the core flooded with SSW with low NaCl concentration ($\sigma_h = 7.0$ MPa). The other cores obtained yield points in the range of 7.6–8.1 MPa; however, without revealing any obvious trend according to the specific flooding fluid. When it comes to strain, it is clearly seen from Fig. 1 that as loading to the pre-set creep stress, the core exposed to SSW deforms more by a factor of 2 than the ones flooded with either DW or NaCl.

When the constant stress level of 10.5 MPa was reached, a creep period followed for each of the cores tested. The axial deformation as a function of time during the creep phase is shown in Figs. 2 and 3. The individual creep periods varied from only 3 days for the core flooded with SSW (RL8) to 3 weeks for one of the two cores flooded with 0.1095 M $MgCl_2$ (RL16). The experimental results achieved during these creep phases are summarized in Table 4. Although the hydrostatic yield point revealed no clear difference between DW, NaCl and $MgCl_2$, the creep data do show an obvious trend. From Fig. 2, it is evident that the creep curves from cores flooded with SSW-like brines (RL8, RL12) and $MgCl_2$ (both high and low concentrations; RL2, RL5, RL16) overlap; the cores show an enhanced deformation compared with the ones exposed to injection of either DW (RL1) or NaCl (RL11, RL14). Plotting the axial creep data versus logarithmic time, a significant difference in strain rates due to

Table 3 Sample ID, porosity values, injected fluid and obtained yield strength

Sample no.	Porosity (%)	Flooding fluid	Yield point (MPa)
RL1	41.4	DW	8.0
RL11	41.2	0.657 M NaCl	7.6
RL14	41.1	0.657 M NaCl	7.8
RL5	41.4	0.1095 M $MgCl_2$	7.8
RL16	41.2	0.1095 M $MgCl_2$	8.1
RL2	41.1	0.219 M $MgCl_2$	7.6
RL8	41.2	SSW	6.6
LR12	41.3	SSW low NaCl conc.	7.0

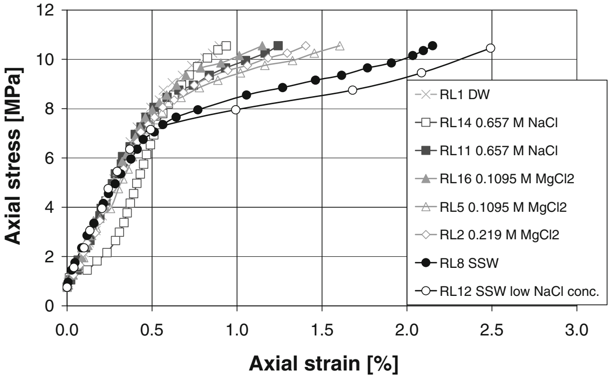

Fig. 1 Axial stress versus axial strain for Liège cores flooded with different fluids at 130°C. Note that the cores flooded with seawater-like brines have significantly lower yield points than those flooded with other fluids

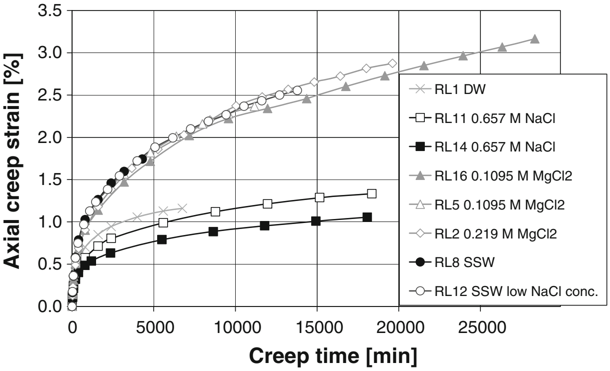

Fig. 2 Axial creep strain versus creep time for Liège cores flooded with different fluids at 10.5 MPa differential creep stress and 130°C. Note that not only the levels of the curves are different, but also the slopes within the steady-state creep

the different chemical compositions of the injected fluids can be noticed (Fig. 3). Obviously, DW and NaCl fall into one group, whereas SSW and $MgCl_2$ follow a completely different trend: the strain rates are increased by a factor of 2 or even more than 3.

One of the cores, RL16, experienced a shut-in period after 5805min of flooding with 0.1095 M $MgCl_2$, resulting in an increase in the strain rate from 1.45 to 1.78 (Table 4). The experiment was ended by a second flooding period and within this last phase the strain rate increased to 2.48%/Decade, i.e. by a factor of 1.7 higher compared to the first flooding phase.

Chalk is known to show a time-dependent behaviour, and the time-dependent effects include consolidation and creep. Consolidation is defined to be the process of draining off an excess pore pressure caused by a change in the effective stress state and is thus represented by the transient phase with respect to the curves in Fig. 3. The period of consolidation varies from 35 to more than 500min for chalk cores flooded with DW and 0.219 M $MgCl_2$, respectively. Flooding with 0.657 M NaCl brine results in a consolidation time of 140min (cores RL11 and RL14). In the case of SSW injection (RL8) or flooding with $MgCl_2$, pore pressure seemed to equilibrate after 313 and 517min, respectively. Hence, these findings point out

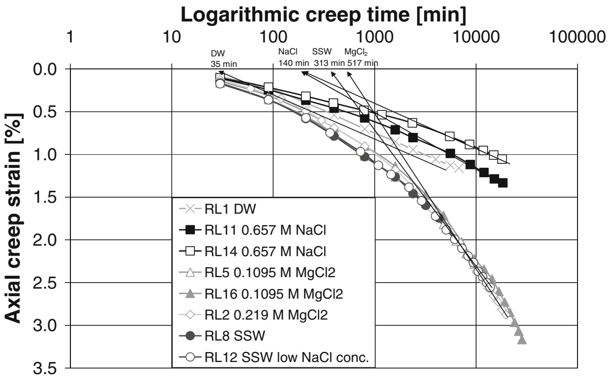

Fig. 3 Axial creep strain versus logarithmic creep time curves for Liège cores flooded with different fluids at 10.5 MPa differential creep stress and 130°C. The intersection of the extended linear line fitted to the curve with the *X*-axis is related to the consolidation time. Cores flooded with $MgCl_2$ brine and SSW-like brines obtain the highest strain rates

Table 4 Sample ID, flooding fluid, flooding periods (min), total (ml) and numbers of pore volume (PV) flooded, total axial strain (%) and strain rates (%/Decade)

Sample no.	Flooding fluid	Creep flooding period (min)		Volume flooded (ml)	PV	Total axial creep strain (%)	*m* (%/ Decade)
		Start (min)	End (min)				
RL1	DW	0	6756	337.8	10.2	1.16	0.51
RL11	0.657 M NaCl	0	18666	429.3	13.0	1.35	0.58
RL14	0.657 M NaCl	0	18078	415.8	12.7	1.06	0.50
RL5	0.1095 M $MgCl_2$	0	11196	257.5	7.8	2.38	1.53
RL16	0.1095 M $MgCl_2$	0	5805	133.5	4.1	1.84	1.45
RL16	No flooding	5805	9561	0.0	0.0	0.39	1.78
RL16	0.1095 M $MgCl_2$	9561	28458	434.6	13.2	0.95 (3.18)[a]	2.48
RL2	0.219 M $MgCl_2$	0	19713	453.4	13.8	2.88	1.78
RL8	SSW	0	4302	98.9	3.0	1.74	1.02[b]
RL12	SSW low NaCl conc.	0	13793	317.2	9.7	2.55	1.49

[a] Total accumulated axial creep strain for RL16 from flooding and non-flooding periods

[b] Test stopped after 4302 minutes of creep due to clogging of chalk core or outlet tubing

that chemistry not only affects the strain rates, but also the time frame of any consolidation process.

4.1.2 Stevns Klint Cores

The Stevns Klint cores are labelled using a letter, e.g. core A. In Table 5, the porosities, aqueous chemistry of the flooding fluid as well as the hydrostatic yield points are given for all the seven Stevns Klint cores tested. In addition, the used pore pressure values are

Table 5 Sample ID, porosity values, injected fluid, pore pressure used and obtained yield strength

Sample no.	Porosity (%)	Flooding fluid	Pore pressure (MPa)	Yield strength (MPa)
Core G	43.36	0.657 M NaCl	0.7	7.5
Core E[a]	42.41	0.657 M NaCl	0.7	7.0
Core M	42.83	0.657 M NaCl	40	7.9
Core C	42.61	0.219 M $MgCl_2$	0.7	9.3
Core P[a]	42.61	0.219 M $MgCl_2$	0.7	6.3
Core A	–	0.219 M $MgCl_2$	40	8.9
Core B	42.37	0.219 M $MgCl_2$	40	9.3

[a] Injection rate: 1 PV/day

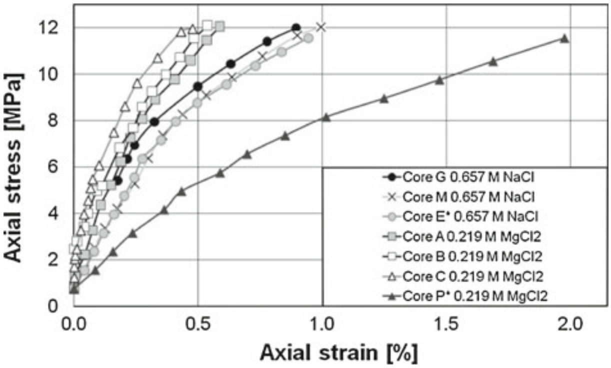

Fig. 4 Axial stress versus axial strain for Stevns Klint cores flooded with different brines at 130°C. Note that core P deformed more by a factor of 2 compared to the other cores flooded with $MgCl_2$. *Square points*: 0.219 M $MgCl_2$, $P_p = 40$ MPa. *Triangular points*: 0.219 M $MgCl_2$, $P_p = 0.7$ MPa. *Cross point*: 0.657 M NaCl, $P_p = 40$ MPa. *Spherical points*: 0.657 M NaCl, $P_p = 0.7$ MPa. *Flooding rate: 1 PV/day

listed. The porosities are approximately 1–2% higher than those of Liège and vary within the range of 42.4–43.4%. Four cores were exposed to 0.219 M $MgCl_2$ brine; two cores (cores C, P) tested at $P_p = 0.7$ MPa and two cores at $P_p = 40$ MPa (cores A, B). For reference purposes, three cores (cores G, M, E) were flooded with NaCl brine with the same ionic strength as the 0.219 M $MgCl_2$ brine used. The flooding rate was in general set to 2 PV/day in this test series; however, the injection rate was reduced to 1 PV/day for two of the samples (cores E, P), which is the same rate as used within the series of Liège cores. As seen from Table 5 and Fig. 4, the values of hydrostatic yield strength, σ_h, are ranging from 6.3 to 9.3 MPa.

Different from Liège, the Stevns Klint cores—with exception of core P—showed a clear trend towards a 20% increase in yield values when comparing all cores exposed to 0.657 M NaCl and 0.219 M $MgCl_2$, respectively. Core P seems to be a very weak core since it differs significantly from the three others exposed to $MgCl_2$, independently of which pore pressure the cores were tested at. It did not only obtain the lowest yield point, but also deformed more by a factor of 2 compared to the other cores flooded with the same brine. Although it could be argued that the lower flooding rate of core P might have caused the reduction in yield strength as well as the enhanced strain within the hydrostatic phase, it seems more likely that this specific core represents a slightly weaker outlier.

After loading beyond yield, a creep period followed for each of the cores tested, lasting for less than 2 days to approximately 2 weeks. Also with respect to the creep phase, the overall picture is at first glance quite different from Liège chalk.

Comparing the series of samples exposed to NaCl and $MgCl_2$, strain rates are reduced by a factor of close to 6 when exposed to $MgCl_2$, independent of the pore pressure used. Then, after 3–8 days of creep at 12.0MPa (approximately 3MPa beyond initiation of pore collapse or yield strength), the two cores flooded with $MgCl_2$ at high pore pressure (cores A, B) showed an unexpected behaviour: creep deformation did start to *accelerate*, which further caused the strain rates to increase by a factor of more than 12, from 0.11 to 1.35%/Decade for core A and 0.12 to 1.38%/Decade for core B (Table 6 and Figs. 5, 6). The shift in strain rates for these two cores thus caused an increase beyond those obtained for the cores exposed to NaCl. Altogether, the observations from these two cores indicate a similar effect of magnesium as observed from the experiments with Liège cores; however,

Table 6 Sample ID, flooding fluid, pore pressure, injection time, total and numbers of pore volume flooded, total axial strain and strain rate

Sample no.	Flooding fluid	Pore pressure (MPa)	Flooding period (min)	Volume flooded (ml)	PV	Total axial strain (%)	*m* (%/Decade)
Core G	0.657 NaCl	0.7	13472	673.6	16.9	1.95	1.12
Core E[a]	0.657 NaCl	0.7	9393	234.8	6.1	1.95	0.99
Core M	0.657 NaCl	40	8407	420.4	10.7	2.16	1.17
Core C	0.219 $MgCl_2$	0.7	7577	378.9	9.7	0.64	0.10
Core P[a]	0.219 $MgCl_2$	0.7	11331	283.3	7.2	2.88	0.36
Core A	0.219 $MgCl_2$	40	9682	340.2	9.6	0.77	0.11 (1.35[b])
Core B	0.219 $MgCl_2$	40	17582	616.6	16.3	0.81	0.12 (1.38[b])

[a] Flooding rate: 1 PV/day
[b] Final strain rate

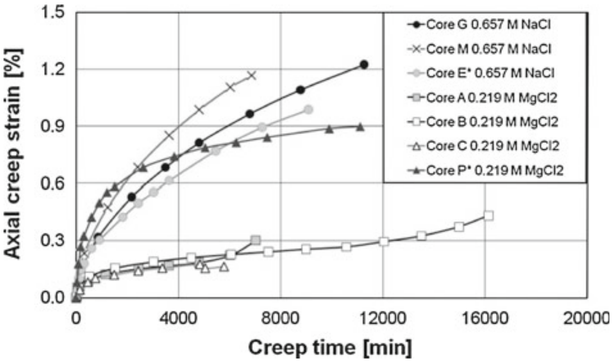

Fig. 5 Axial creep strain versus creep time for Stevns Klint cores flooded with different brines at 12.0 and 11.3MPa (cores P and E) effective creep stress at 130°C. Note the *accelerating creep* behaviour for cores flooded with $MgCl_2$ brine at high pore pressure (cores A and B). *Square points*: 0.219 M $MgCl_2$, $P_p = 40$ MPa. *Triangular points*: 0.219 M $MgCl_2$, $P_p = 0.7$ MPa. *Cross point*: 0.657 M NaCl, $P_p = 40$ MPa. *Spherical points*: 0.657 M NaCl, $P_p = 0.7$ MPa. *Flooding rate: 1 PV/day

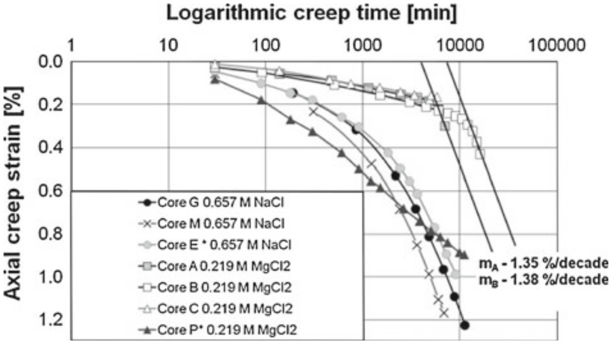

Fig. 6 Axial creep strain versus logarithmic creep time for Stevns Klint cores flooded with different brines at 12.0 and 11.3MPa (cores P and E) effective creep stress at 130°C. Accelerating creep is observed for cores A and B which were both flooded with $MgCl_2$ at high pore pressure. *Square points*: 0.219 M $MgCl_2$, $P_p = 40$ MPa. *Triangular points*: 0.219 M $MgCl_2$, $P_p = 0.7$ MPa. *Cross point*: 0.657 M NaCl, $P_p = 40$ MPa. *Spherical points*: 0.657 M NaCl, $P_p = 0.7$ MPa. *Flooding rate: 1 PV/day

the enhanced creep caused by $MgCl_2$ injection is somewhat delayed and also the degree of weakening is significantly less with Stevns Klint chalk.

4.2 Chemical Analyses of the Sampled Effluents

The flooding effluent from each mechanical test was generally sampled during the entire test period; i.e. prior to and during any isotropic or hydrostatic loading, and during creep. The ionic concentrations were analysed by an ion-exchange chromatograph, Dionex ICS-3000 produced by Dionex Corporation, Sunnyvale, CA, USA. The analyses were performed isocratic with a conductivity detector, ICS 3000 CD Conductivity Detector. IonPac AS16 and IonPac CS12A were used as anion and cation exchange columns, respectively. The sampled effluents were diluted to stay in the linear region of the calibration curve and the ionic concentrations were calculated based on an external standard method. Some additional water samples were fractioned and submitted to a commercial laboratory for inductively coupled plasma optical emission spectrometer (ICP-OES) analysis, VISTA-PRO CCDS Simultaneous ICP-OES produced by Varian Inc. ICP-OES provides total elemental analysis of a chemical solution or materials in aqueous solution. The analyses (Table 7) conducted by Eurofins Norsk Miljøanalyse AS were performed on both types of chalk tested and generally confirm the results of this study gained from the IC-analyses.

Table 7 ICP-OES analyses of the fractioned effluent from two chalk cores; Liège and Stevns Klint, flooded with 0.219 M $MgCl_2$ and 0.1095 M $MgCl_2$, respectively

Chalk type	Brine	Sampling time (min)	Ca^{2+} (mol/l)	Mg^{2+} (mol/l)	Si (mol/l)	Total Mg^{2+} and Ca^{2+} (mol/l)
Liege	0.219 M	369	0.072	0.178	0.0021	0.250
	$MgCl_2$	7348	0.050	0.186	0.0024	0.236
		17408	0.035	0.205	0.0024	0.240
Stevns Klint	0.1095 M	132	0.030	0.095	0.0016	0.125
	$MgCl_2$	2889	0.027	0.099	0.0016	0.126
		6958	0.020	0.103	0.0013	0.123

4.2.1 *Liège Cores*

The chemical analyses of the effluent fractioned during injection of DW confirmed the presence of only a minor amount of Ca^{2+} ions, i.e. 0.003 mol/l. Within the start-up of any flooding, the effluent will be a mixture of distilled water and the actual brine, since all cores are saturated with DW from the beginning. When flooding with NaCl (core RL11), it takes less than 1000 min before Na^+ and Cl^- ions reach their original concentrations; thereafter, these values stay close to constant during the remaining injection period (Fig. 7). Some calcium is produced, 0.01 mol/l within the first 1000 min, subsequently decreases and reaches a constant value of 0.004 mol/l throughout the experiment.

The chemical analyses from the three cores flooded with $MgCl_2$ also show that chloride seems to be more or less inert to the chalk surface, since it rapidly reaches its original concentration. All cores exposed to $MgCl_2$ injection do, however, experience a significant loss of magnesium inside the core, while at the same time a considerable amount of calcium is produced. During the entire testing period, the concentration of Ca^{2+} ions detected in the effluent is higher than the Ca^{2+} concentration as present in seawater; moreover, the concentration of Mg^{2+} ions never reaches that of the injected brines, i.e. 0.1095 M (Fig. 8) or 0.219 M $MgCl_2$ (Fig. 9), respectively.

The observed changes in the ionic concentrations gained from the IC analyses of this study were further confirmed by additional ICP-OES analyses (Table 7). These recent analyses also showed a significant amount of silicon, 2.4×10^{-3} mol/l, was detected within the

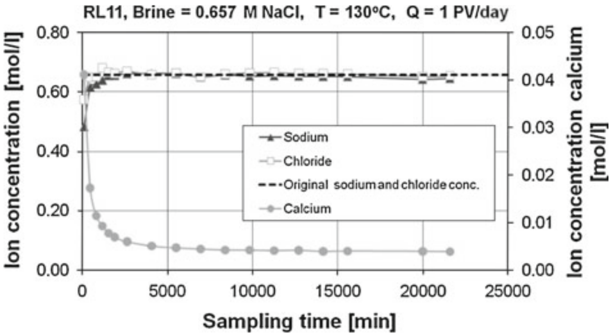

Fig. 7 Na^+, Cl^- and Ca^{2+} concentrations in sampled effluents from core RL11, flooded with 0.657 M NaCl. Ca^{2+} concentration presented in the secondary *y*-axis. Sampling time started when 130°C were reached

Fig. 8 Mg^{2+}, Ca^{2+} and Cl^- concentrations in sampled effluents from core RL5, flooded with 0.1095 M $MgCl_2$. Sampling time started when 130°C were reached

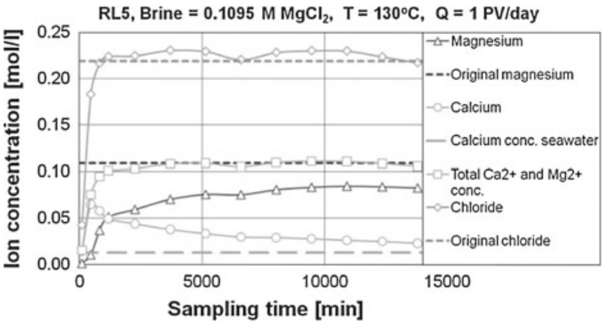

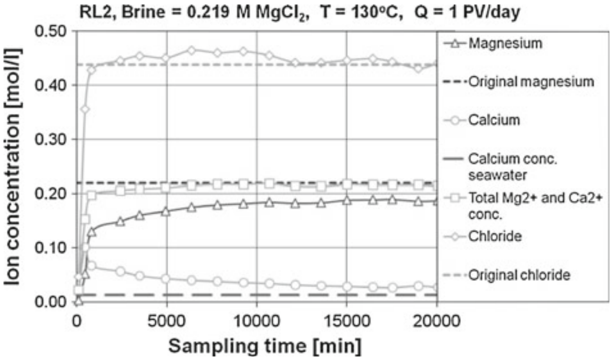

Fig. 9 Mg^{2+}, Ca^{2+} and Cl^- concentrations in sampled effluents from core RL2 flooded with 0.219 M $MgCl_2$. Sampling time started when 130°C were reached

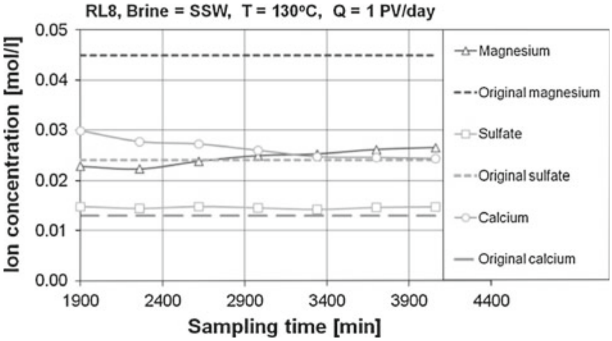

Fig. 10 Mg^{2+}, Ca^{2+} and $SO_4{}^{2-}$ concentrations in sampled effluents from core RL8 flooded with SSW. Sampling time started when 130°C were reached

fractioned effluent. These additional findings show that not only calcium, but also silicon is being produced when flooding with $MgCl_2$ at 130°C.

For the cores flooded with SSW-like brines, the Mg^{2+} and Ca^{2+} concentrations did change in the same manner as observed for the cores flooded with $MgCl_2$ brines. In core RL8, a large reduction in the Mg^{2+} concentration was detected; lower by a factor of 1.7 to 2 than its original Mg^{2+} concentration (Fig. 10). The increase in Ca^{2+} concentration was even higher, by a factor of 1.8 to 2.3 compared to the original concentration. When flooding core RL8 with SSW at 130°C, a reduction in the $SO_4{}^{2-}$ concentration from 0.024 mol/l to a constant value of approximately 0.014 mol/l was detected (Fig. 10). This reduction in $SO_4{}^{2-}$ ions, in addition to the clogging of the core itself after 3 days of SSW injection, points towards precipitation of anhydrite, $CaSO_4$ (Heggheim et al. 2005; Hiorth et al. 2008a, b, 2010; Madland et al. 2008). This assumption is further strengthened by summing up the additional amount of Ca^{2+} ions in the effluent and the measured Mg^{2+} concentration. Total Mg^{2+} and Ca^{2+} concentration is now lower than the original Mg^{2+} concentration prior to flooding. In the previous tests involving flooding of low and high concentration $MgCl_2$ brines, the trend seems to be that this value generally adds up to the original Mg^{2+} concentration after 2–3 days flooding when steady-state values are reached.

4.2.2 Stevns Klint Cores

Chemical analyses of the fractioned effluent similar to those performed for the Liège cores were also carried out for the Stevns Klint cores. Also with Stevns Klint chalk, calcium is being produced throughout the flooding periods; however, from the cores flooded at a pore pressure of 0.7MPa a somewhat lower concentration of Ca^{2+} is detected within the fractioned effluent. Still, Ca^{2+} production seems to stabilize around the concentration as present in seawater, 0.013 mol/l (Fig. 11). As pore pressure is increased to 40MPa, slightly more Ca^{2+} seems to be produced. Independent of which pore pressure the Stevns Klint cores were flooded at, somewhat less Mg^{2+} is retained compared to the observations made from the Liège cores, compare, e.g. Figs. 11, 12 and Fig. 9. Nevertheless, the concentration of Mg^{2+} never reaches that of the injected brine, 0.219 M $MgCl_2$.

Some additional ICP-OES analyses (Table 7) were conducted for Stevns Klint chalk as well and in general showed similar results as those obtained from our own IC-analyses.

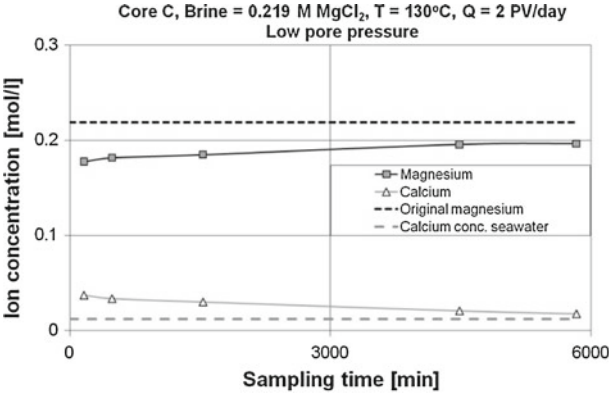

Fig. 11 Chemical analyses of sampled effluents from core C, flooded with 0.219 M $MgCl_2$ at low pore pressure. Cl^- concentration was not measured. Isotropic loading started at sampling time zero

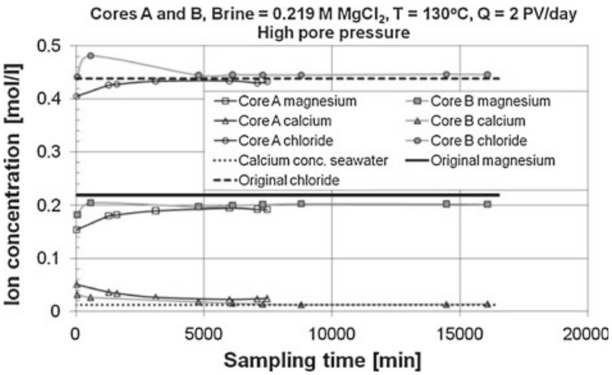

Fig. 12 Chemical analyses of sampled effluents from cores A and B flooded with 0.219 M $MgCl_2$ at high pore pressure. Mg^{2+}, Ca^{2+} and Cl^- concentrations were identified for both cores. Isotropic loading started at sampling time zero

Also in these additional analyses, silicon was detected within the fractioned effluent, in the order of 1.0×10^{-3} mol/l, indicating that also this more pure chalk exhibits some dissolution of silicates when flooding with $MgCl_2$ at elevated temperature.

4.3 Modelling Results

Motivated by the experimental results, we wanted to explore whether the observed ionic concentrations at the outlet end could be explained as a result of interplay between transport effects (convection and molecular diffusion) and precipitation/dissolution of minerals. For this purpose, we propose a 1D mathematical model which is composed of convection–diffusion–reaction equations for the aqueous species in question, and appropriate ordinary differential equations for the relevant mineral species. The authors present simulation results from $MgCl_2$ flooding at 130°C. In particular, we include calcite, magnesite and anhydrite and various ions relevant for dissolution/precipitation of these minerals. The model of this study does not yet include processes involving dissolution and reprecipitation of silicates; however, these will be incorporated at a later stage. For details as far as the mathematical model is concerned, we refer to a study by Evje et al. (2009). The approach we use is similar to, for example, the recent study by Bouillard et al. (2007), who studied precipitation/dissolution in a simplified system composed of one mineral and two aqueous species. We basically follow along the line of the study by Steefel and Lasaga (1994).

The model of this study is solved numerically by using an operator splitting approach where convection and diffusion effects for the aqueous species are accounted for in a separate step, followed by another step where a coupled system of ordinary differential equations is solved that accounts for the dissolution/precipitation effects. It should be noted that since the chemical changes of Ca^{2+} and Mg^{2+} in general did not show any significant difference for the two outcrop chalks tested, any comparison of the experimental results with those obtained from simulations had been performed using the chemical analyses of effluents collected from the Liège cores.

We refer to the study by Evje et al. (2009) for details concerning the rate laws, kinetic constants, as well as thermodynamic constants that have been used. The way we use the model for comparison with the experiments is as follows: it is assumed that the fluid (containing the various ions) is transported at a constant velocity calculated from the known injection rate, 1 PV/day. The total diffusion effect, that is, the sum of the molecular diffusion and the mechanical dispersion, is set to be $10^{-8}\,\mathrm{m}^2/\mathrm{s}$. The model then produces a profile for the chloride concentration at the outlet that agrees well with the experimental profile (see Figs. 13, 14). According to the experimental observations, it is assumed that chloride is not involved in the chemical reactions (see also Evje et al. 2009).

We can then choose reaction rate constants for the precipitation/dissolution process associated with $CaCO_3$ and $MgCO_3$ such that the outlet profiles of the concentration of Ca^{2+} and Mg^{2+} fit well with the corresponding experimental profiles; at least, when a steady value had been reached.

The results of the example with a 0.1095-M $MgCl_2$ brine are shown in Fig. 13. In a second simulation, we double the concentration and consider a brine of 0.219 M $MgCl_2$. We use the same parameters (fluid velocity, molecular diffusion and reaction rate constants) as for the first example and compute concentrations at the outlet end (Fig. 14). The results demonstrate that the model is able to capture well the basic mechanisms as reflected in the experimental results, illustrated in Figs. 8 and 9. We may thus conclude, based on the example

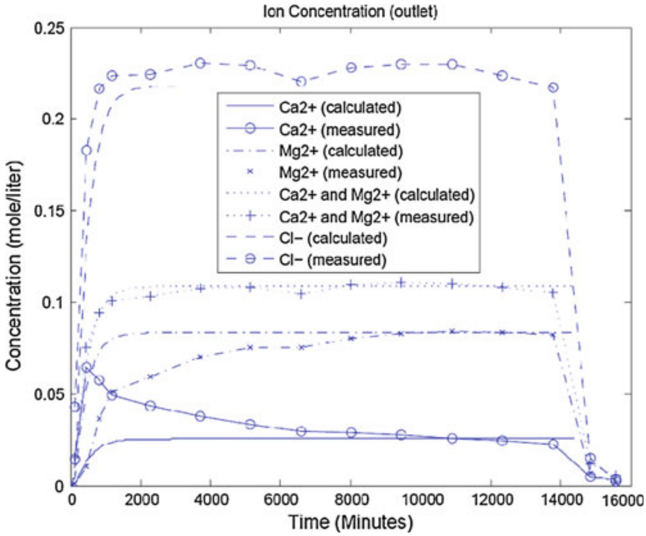

Fig. 13 Simulated and measured concentration for a chalk core flooded with a 0.1095-M $MgCl_2$ brine. Note that the model captures well the Cl^- concentration and the long-term Mg^{2+} and Ca^{2+} concentrations. The model initially overpredicts the magnesium concentration and predicts a too low value for the calcium concentration. This is because the fact that the model does not take into account the ion exchange capacity of the core

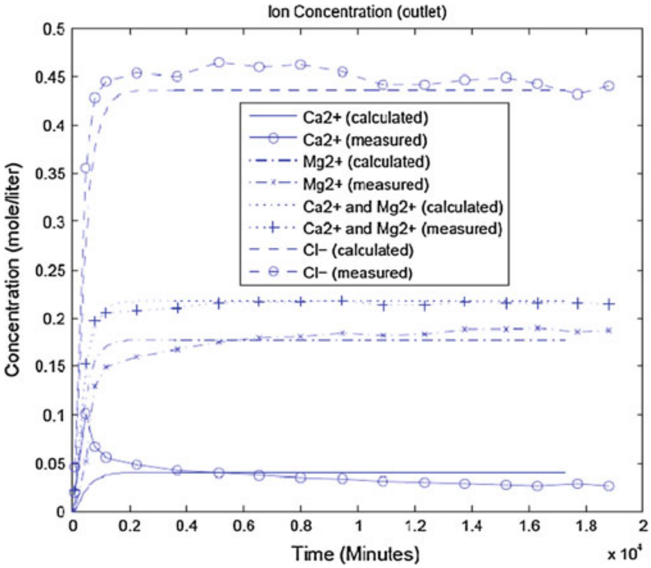

Fig. 14 Simulated and experimental results for a chalk core flooded with a 0.219-M $MgCl_2$ brine. As shown in Fig. 13, the model fits nicely with the steady-state results, but gives a poor fit within the first day of flooding. This is because the fact that ion exchange is not included in the model. Note, however, that the model generally matches the measured sum of magnesium and calcium

with flooding of $MgCl_2$, that the model seems to offer a sound basis for further systematic investigations of possible precipitation/dissolution processes relevant for chalk-weakening effects.

5 Discussion

There seems to be a clear physical response when the cores are subjected to different aqueous chemistry. This corresponds to the results reported previously by Korsnes et al. (2006a, b). In Fig. 15, we have plotted the final strain rate and yield strength for all cores tested (Tables 3, 4, 5, 6) as a function of the magnesium concentration in the injected brine. For the Liège cores, there is a strong correlation between the amount of magnesium present in the invading brine and the strain rate. The strain rate increases with increased concentration of magnesium. For the series of Stevns Klint cores, there is a similar correlation; however, only if considering the final values of strain rates for the two cores flooded at high pore pressure; A and B. The values of yield point obtained from the Liège cores do not reveal any effects due to the presence of magnesium; however, in the case of Stevns Klint, except for core P, the hydrostatic yield increases with increasing magnesium concentration.

One of the hypotheses from earlier study has been that magnesium substitutes calcium inside the core material, by the help of sulphate. In this study, we have clearly demonstrated that sulphate is not needed to have a significant amount of chemical deformation. A large deformation, comparable with deformation caused by SSW, is seen in the cases where only $MgCl_2$ was present in the fluid. Nonetheless, a substitution process without sulphate cannot

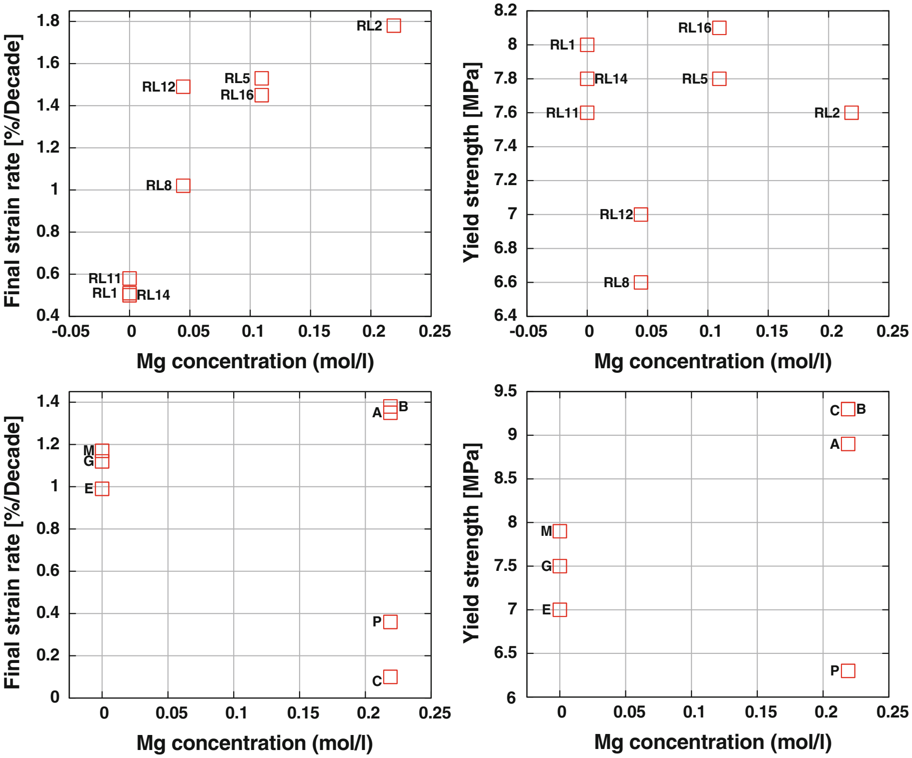

Fig. 15 Mechanical test results as a function of magnesium concentration in the flooding fluid. *Upper left*: Mg^{2+} versus strain rates for Liège cores. *Upper right*: Mg^{2+} versus hydrostatic yield points for Liège cores. *Lower left*: Mg^{2+} versus final strain rates for Stevns Klint cores. *Lower right*: Mg^{2+} versus hydrostatic yield points for Stevns Klint cores

be ruled out. To further investigate the substitution hypothesis as presented by Korsnes et al. (2006a, b), we base the following discussion on the data containing $MgCl_2$ only. From the data shown in Figs. 13 and 14, it is obvious that a significant amount of magnesium is lost inside the core and additionally calcium is produced. The added calcium and magnesium concentrations are more or less constant and equal to the concentration of $MgCl_2$ injected. This might indicate a substitution process inside the core, as quantitatively, there seems to be a one-to-one exchange of magnesium and calcium. To pursue the substitution mechanism somewhat further, we can evaluate how many mol of magnesium are lost in this core, by simply summing up the amount of magnesium lost during the experiment:

$$V_{\mathrm{PV}} \int_{1}^{9} \left(m_{\mathrm{Mg}^{2+}}^{\mathrm{in}} - m_{\mathrm{Mg}^{2+}}^{\mathrm{out}} \right) \mathrm{d}V_{\mathrm{PV}} \approx 0.01 \mathrm{mol}. \tag{2}$$

The calculated loss is based on the experimental data in Fig. 13. This number is approximately five times greater than the largest possible adsorption that could take place inside the core, which we calculated to be about 0.0019 mol (see Eq. 1). If the experiment had been continued, an even greater loss of magnesium would have occurred, since steady state was not reached in the course of the experiment. The amount of magnesium lost is too high to be a consequence of substitution alone. Another possibility of losing magnesium inside the core is the precipitation of magnesium as part of a new mineral phase. Theoretically, we assume that the fluids tend to equilibrate chemically with the core minerals. According to equilibrium calculations performed using EQAlt (L. M. Cathles, unpublished data), several minerals are supersaturated as a chalk core is flooded with 0.219 M $MgCl_2$ at the temperature and pressure the experiment was run at ($T = 130°\mathrm{C}$ and $P = 0.7\,\mathrm{MPa}$) (see Table 8).

The calculations indicate that the solution is greatly supersaturated with respect to huntite (Table 8). Recalculating with huntite as a buffer mineral, we find that the equilibrium concentration of calcium and magnesium is 1.23×10^{-1} mol/l and 9.47×10^{-2} mol/l, respectively. These calculations thus confirm that much of the calcium present in the effluent has to be supplied from the rock in order for the rock to be in equilibrium with a fluid containing $MgCl_2$ only. The interesting observation here is that even if the pH of the injected fluid is close to neutral, the injected fluid can cause significant dissolution of the rock. The explanation for this is that when minerals like huntite are being precipitated, the fluid loses calcium (or carbonate), which must then be replaced from the rock to approach equilibrium,

Table 8 Supersaturated minerals when a chalk core is flooded with 0.219 M $MgCl_2$ at 130°C and 0.7MPa; calculations were performed using EQAlt and assume equilibrium with calcite and CO_2(g) at a partial pressure of $10^{-3.5}$

Mineral	Log_{10} Q/K EQAlt	Log_{10} Q/K PHREEQC
Huntite	5.25	7.50
Hydromagnesite	4.13	9.90
Dolomite	3.25	4.00
Brucite	2.46	3.62
Magnesite	2.09	2.84
Artinite	0.94	4.04

As a comparison PHREEQC (Parkhurst and Appelo 1999) calculations are shown using the llnl database at 130°C and 0.1MPa (there is no pressure-dependent database in PHREEQC) thus inducing calcite dissolution. Our calculations also show that there are significant rate effects. The experimental data obtained from Liège cores deforming at a creep stress level equal to 10.5MPa show steady-state level of calcium equal to 0.02 mol/l; however, the cores reached only approximately $0.02/0.123 = 16\%$ of equilibrium. The chemical analyses of the collected effluent from the Stevns Klint creep experiments performed at a somewhat higher effective stress level, 12MPa and with $P_\mathrm{p} = 0.7$ MPa, seem to show even lower concentration of calcium at steady state, which may indicate that these cores require an extended time before equilibrium is reached. A comparison of the two sets of experiments conducted at low pore pressure shows that the Stevns Klint cores reached an even lower equilibrium percentage, 10%, while flooding, although these experiments were carried out at a somewhat higher effective stress, 1.5MPa, and flooding rate, 2 PV/day, compared to the Liège cores. It should be noted that the other Stevns Klint cores performed at the very same effective stress level of 12MPa, but at a higher pore pressure ($P_\mathrm{p} = 40$ MPa), produced in general as much calcium as the Liège cores. One may argue that an increased pore pressure will cause the injected fluid to be more evenly distributed within the chalk matrix and thus also may cause several surface sites available for dissolution.

The effect of pore pressure is not clearly understood, but increasing the pore pressure seems not only to influence any chemical changes in the ionic composition of the fractioned effluent, but also the development of the creep behaviour. Two of the cores flooded at high pore pressure showed an unexpected mechanical behaviour: accelerating creep or tertiary creep. After approximately 3–8 days of creep, deformation rapidly increased for cores A and B, and strain rates thus showed an increase by a factor of more than 12 (Figs. 5, 6).

In Fig. 16, both the creep strain and the calcium concentration of the fractioned effluent are plotted versus creep time for cores A and B. Core A (denoted with triangular points) shows a clear tendency towards an increase in calcium production as creep starts to accelerate. Also for core B the same trend is observed, however, less distinct.

The total axial strain for the $MgCl_2$ flooded cores is significantly lower than the total strain of the NaCl flooded cores (see Table 6 and Figs. 5, 6). However, if the two cores showing accelerating creep had been allowed to continue for a longer time, then they may have reached the same value of axial strain as the cores exposed to NaCl. The evident effect of magnesium as first observed from the experiments with Liège chalk, also seems to be of importance as discussing the chemical weakening of the more pure Stevns Klint outcrop chalk. The time

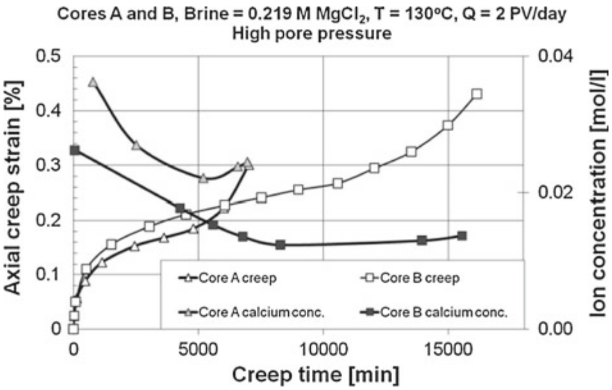

Fig. 16 Axial creep strain and ion concentration of the fractioned effluents versus creep time for cores A and B. Note increased Ca^{2+} production when creep accelerates

frame of the experiments is, however, an issue. In case of the Stevns Klint chalk, it seems like magnesium requires a somewhat longer time in order to react and thus precipitate as a new mineral phase, which further seems to cause a similar although less pronounced difference in strain rates when compared to the series of Liège cores. Although core P is considered to be a very weak core, a comparison of the two Stevns Klint cores exposed to $MgCl_2$ at low pore pressure might indicate a certain effect of flooding rate: Core P, which is flooded at half the rate of core C, not only obtains the lowest yield point and enhanced strain within the loading phase, but the strain rate within the following creep phase is additionally increased by a factor of more than 3 compared to core C. To better understand the possible effects when varying the injection rate, we recently started a systematic study that will validate rates of reactions used in our model and the interplay between transport effects and reactions itself.

So far any chemical changes and mineralogical alterations discussed were predicted based on very simple core chemistry. A buffer system that includes aluminosilicate minerals, however, suggests that alteration may be more extensive and involve other than carbonate minerals. A study by Hjuler and Fabricius (2009) showed that the two investigated types of outcrop chalk have a slightly differing mineralogy: Stevns Klint chalk is a particularly pure calcium carbonate rock with as little as 0.2 wt% non-carbonate minerals, whereas Liège chalk typically contains approximately 1.9 wt% (0.95 wt% quartz, 0.19 wt% smectite, 0.19 wt% mica and 0.57 wt% clinoptilolite). These silicate minerals can react with the brine, inducing a more complex alteration when $MgCl_2$ is injected into chalk cores than previously considered.

The computed mineral alteration is very sensitive to the buffer minerals chosen and to their stoichiometry. For the alteration to be computed accurately, it will be important to determine the actual stoichiometry of all minerals (original and secondary) within the chalk considered. This will be a future objective for a petrographic study. However, for the time being, the most critical objective has been to investigate if the predicted mineral alterations can be verified. It has been of special interest whether magnesium-bearing minerals as well as anhydrite could be detected in the chalk when altered by injecting $MgCl_2$ or seawater at 130°C, and additionally to assess the extent of possible aluminosilicate modification.

Future work will also include pore-scale Lattice Boltzmann simulations which will quantify the changes on the pore scale, such as the chemistry of the fluid while matrix changes occur, wettability, mineral dissolution and precipitation, and how the permeability of the matrix will change. These pore-scale results will then be incorporated into our core-scale model.

5.1 Evidence of Mineral Precipitation

Our core-scale model, which is based on experimental observations, suggests mineral dissolution and precipitation in chalk that is flooded with certain brines at elevated temperature. Precipitation of supersaturated minerals in connection with enhanced dissolution of calcite is therefore expected. To verify the predicted precipitation of new minerals in the chalk matrix, some cores flooded with $MgCl_2$ brine and SSW with low NaCl concentration had subsequently been studied using scanning electron microscopy with X-ray microanalysis (SEM-EDS). For comparison, the core flooded with DW only (RL1) was additionally analysed.

The analyses revealed very low magnesium contents of <0.25 wt%, i.e. close to the detection limit, in the chalk core flooded with distilled water. The grains appeared relatively clean, even though some silicates covering the grain surfaces could be noticed (Fig. 17). SEM-EDS bulk measurements after flooding with $MgCl_2$ indicate that the brine had caused a manifold

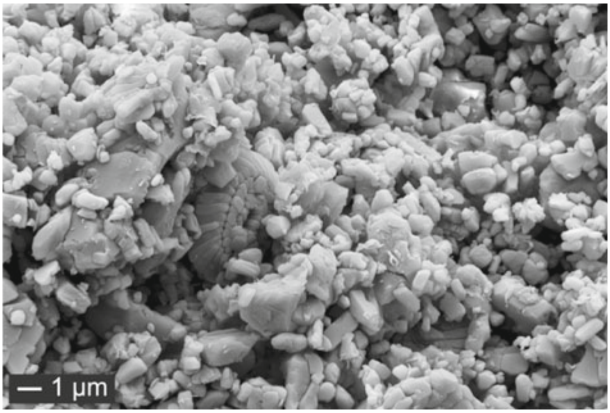

Fig. 17 SEM micrograph of chalk core RL1 after flooding with distilled water; note relatively clean calcite grain surfaces with only minor amounts of silicates

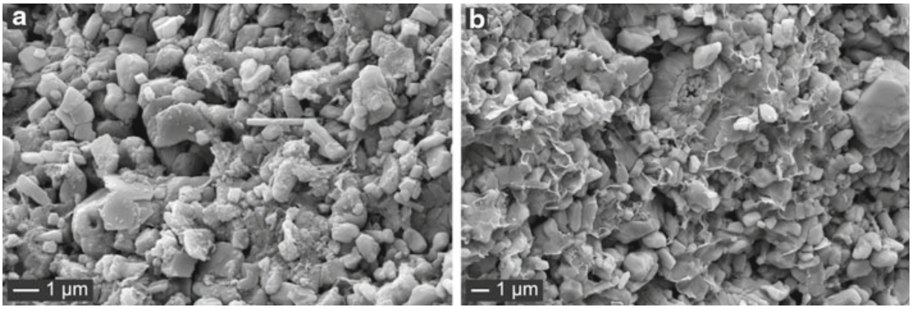

Fig. 18 SEM micrographs of chalk core RL16 showing different magnesium-bearing precipitates after flooding with 0.1095 M $MgCl_2$; **a** calcite grains covered with aggregates of tiny (carbonate?) minerals; **b** calcite grains covered with clay-like (silicate?) minerals

increase in the amount of magnesium in the chalk matrix. The chalk appears altered, and supposedly different types of precipitated minerals cover the grain surfaces (Fig. 18). From the element analyses, it is obvious that magnesium is retained particularly in the newly formed minerals, and not so much in the calcite grains themselves.

Even though the exact nature of the precipitates formed from flooding with $MgCl_2$ brine presently remains undetermined, more detailed SEM-EDS analysis suggests that at least two different types of newly precipitated magnesium-bearing minerals are present: a possible silicate mineral with a clay-like appearance, containing silicon in addition to magnesium and resulting from the dissolution of silicates present in the chalk, and one or more magnesium-bearing carbonate minerals. Additional data from a $MgCl_2$ flooded Stevns Klint chalk core indicate that huntite, $CaMg_3(CO_3)_4$, (unpublished SEM-EDS data, T. Hildebrand-Habel, 2009) and/or magnesite, $MgCO_3$, (unpublished X-ray diffraction data, SINTEF report, R. Bøe, 2009) might have been precipitated.

Flooding of SSW with low NaCl concentration resulted in the precipitation of both magnesium-bearing minerals comparable to those illustrated in Fig. 18 and the formation of anhydrite, $CaSO_4$. Anhydrite precipitated as bladed or platy crystals aggregating to larger masses and locally filling significant portions of the pore space (Fig. 19).

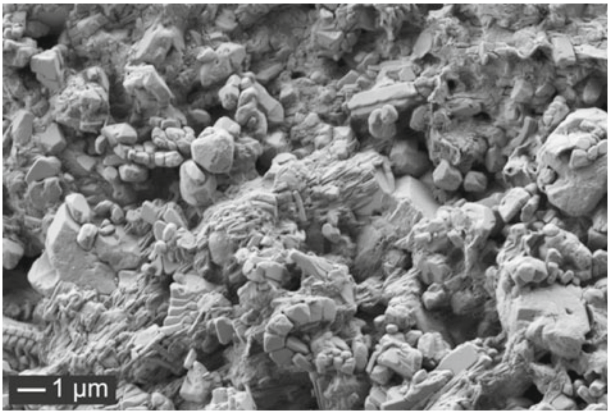

Fig. 19 SEM micrograph of chalk core RL12 after flooding of SSW with low NaCl concentration; aggregates of bladed-massive anhydrite precipitates partly fill the pore space

6 Conclusions

When analysing the effluent fractioned from all the samples independently of chalk type, we observe that excess calcium is being produced both in the case of seawater-like and $MgCl_2$ brines as an injection fluid. In light of these new results, we discuss the Ca–Mg substitution mechanism as suggested by Korsnes et al. (2006a, b). This substitution mechanism cannot be the full explanation for the observed results, simply because we observe a greater production of calcium and retention of magnesium than what is reasonable to expect from calculations. We performed equilibrium calculations, showing that huntite is the most likely mineral to be formed inside the core. We suggest that the precipitation of new minerals leads to a significant dissolution, which surely, all depending on where these processes are taking place within the core, may cause an enhanced weakening of the chalk framework itself. The formation of different magnesium-bearing minerals as chalk cores are exposed to $MgCl_2$ injection was verified by SEM-EDS analyses, substantiating the influence of precipitation–dissolution processes, even though the exact nature of the formed precipitates still remains uncertain. When seawater-like brine was flooded, not only the precipitation of magnesium-bearing minerals, but also the formation of anhydrite, $CaSO_4$, was detected. From the flooding experiments, we estimate the rate effects to be of the order of approximately 16% or even less; i.e. the fluid reaches not more than 16% of the equilibrium calcium concentration. From the mechanical tests on Liège cores, we showed that injection of brine-containing magnesium only makes the chalk deform similar to exposure to seawater. Obviously, the weakening is not caused by substitution of calcium by magnesium in the presence of sulphate. The increased strain rates that the cores exposed to seawater and $MgCl_2$ experience compared with the ones exposed to NaCl and DW must be of chemical nature.

The degree of water weakening seems not only to be governed by the ionic compositions of the injected brines, but also the purity of the chalk cores tested. Other non-carbonate minerals originally present in the chalks seem to have an important impact on the chemical weakening taking place. A 1D model that simulates the time-dependent chemical changes was developed, and it gives excellent fit to the measured retention of magnesium and production of calcium during the progressing flooding experiment. The observed chemical changes are interpreted in terms of mineral dissolution and precipitation. We would like to point out, however, that the dissolution of the chalk core may not (yet) directly be linked to the weakening of the chalk matrix, even though this seems a likely explanation. In addition, any effects of surface charge on the chalk matrix should be evaluated in future studies; it is important to understand the significance of the short range forces that probably play a major role in determining the strength of chalk.

Acknowledgments The authors acknowledge the Norwegian Research Council, ConocoPhillips and the Ekofisk co-venturers, including TOTAL, ENI, Statoil and Petoro, as well as BP and the Valhall co-venturers, including Hess Norge AS, A/S Norske Shell and Total E&P Norge AS, for financial support for this study.

References

Bouillard, N., Eymard, R., Herbin, R., Montarnal, P.: Diffusion with dissolution and precipitation in a porous medium: mathematical analysis and numerical approximation of a simplified model. M2AN **41**(6), 975–1000 (2007)

Davis, J.A., Kent, D.B.: Surface complexation modeling in aqueous geochemistry. Rev. Mineral. Geochem. **23**(1), 177–260 (1990)

Evje, S., Hiorth, A, Madland, M.V., Korsnes, R.I.: A mathematical model relevant for weakening of chalk reservoirs due to chemical reactions networks and heterogeneous media. Netw. Heterog. Media **4**(4), 755–788 (2009)

Heggheim, T., Madland, M.V., Risnes, R., Austad, T.: A chemical induced enhanced weakening of chalk by seawater. J. Pet. Sci. Eng. **46**, 171–184 (2005)

Hiorth, A., Cathles, L.M., Kolnes, J., Vikane, O., Lohne, A., Madland, M.V.: Chemical modelling of wettability change in carbonate rocks. In: 10th Wettability Conference, Abu Dhabi, UAE, pp. 1–9 (2008a)

Hiorth, A., Cathles, L.M., Kolnes, J., Vikane, O., Lohne, A., Korsnes, R.I., Madland, M.V.: A chemical model for the seawater-CO_2-carbonate system—aqueous and surface chemistry. In: International Symposium of the Society of Core Analysts, Abu Dhabi, UAE, SCA2008-18, pp. 1–12 (2008b)

Hiorth, A., Cathles, L.M., Madland, M.V.: The impact of pore water chemistry on carbonate surface charge and oil wettability. Transp. Porous Med. doi:10.1007/s11242-010-9543-6 (2010)

Hjuler, M.L., Fabricius, I.L.: Engineering properties of chalk related to diagenetic variations of Upper Cretaceous onshore and offshore chalk in the North Sea area. J. Pet. Sci. Eng. **68**, 151–170 (2009)

Korsnes, R.I.: Chemical induced water weakening of chalk by fluid-rock interaction. A mechanistic study. PhD thesis, University of Stavanger. ISBN 978-82-7644-316-5. ISSN 1890-1387 (2007)

Korsnes, R.I., Strand, S., Hoff, Ø., Pedersen, T., Madland, M.V., Austad, T.: Does the chemical interaction between seawater and chalk affect the mechanical properties of chalk? In: Cottheim, A.V., Charlier, R., Thimus, J.F., Tshibangu, J.P. (eds.) Eurock 2006a, Multiphysics Coupling and Long Term Behaviour in Rock Mechanics, pp. 427–434. Taylor & Francis, London (2006a)

Korsnes, R.I., Madland, M.V., Austad, T. : Impact of brine composition on the mechanical strength of chalk at high temperature. In: Cottheim, A.V., Charlier, R., Thimus, J.F., Tshibangu, J.P. (eds.) Eurock 2006b, Multiphysics Coupling and Long Term Behaviour in Rock Mechanics, pp. 133–140. Taylor & Francis, London (2006b)

Korsnes, R.I., Madland, M.V., Austad, T., Haver, S., Røsland, G.: The effects of temperature on the water weakening of chalk by seawater. J. Pet. Sci. Eng. **60**(3–4), 183–193 (2008)

Madland M.V.: Water weakening of chalk. A mechanistic study. PhD thesis, University of Stavanger. ISBN 82-7644-257-9. ISSN 1502-3877 (2005)

Madland, M.V., Midtgarden, K. Manafov, R. Korsnes, R.I. Kristiansen, T.G., Hiorth, A.: The effect of temperature and brine composition on the mechanical strength of Kansas chalk. In: International Symposium of the Society of Core Analysts, Abu Dhabi, UAE, SCA2008-55, pp. 1–6 (2008)

Parkhurst, D.L., Appelo, C.A.J.: User's guide to PHREEQC (version 2)—A computer program for speciation, batch-reaction, one-dimensional transport, and inverse geochemical calculations. US Geol. Survey, Water-Resour. Invited Report, 99-4259 (1999)

Puntervold, T., Strand, S., Austad, T.: New method to prepare outcrop chalk cores for wettability and oil recovery studies at low initial water saturation. Energy Fuels **21**(6), 3425–3430 (2007)

Steefel, C.I., Lasaga, A.C.: A coupled model for transport of multiple chemical species and kinetic precipitation/dissolution reactions with application to reactive flow in single phase hydrothermal systems. Am. J. Sci. **294**, 529–592 (1994)

Zangiabadi, B., Korsnes, R.I., Hildebrand-Habel, T., Hiorth, A., Surtarjana, I.K., Lian, A., Madland, M.V.: Chemical water weakening of various outcrop chalks at elevated temperature. In: Ling, H.I., Smyth, A., Betti, R. (eds.) Poromechanics IV: Proceedings of the 4th Biot Conference on Poromechanics, pp. 543–548. DEStech Publication, Inc., PA, USA (2009)